

Shelling Tumors with Caution and Wiggles

Luke Winstrom

Sam Coskey

Mark Blunk

University of Washington
Seattle, WA

Advisor: James Allen Morrow

Abstract

We discuss a simple model for tumor growth, which results in realistic tumor shapes. We then address the question of efficient irradiation of tumors in terms of packing their volume with disjoint spheres of given radii. We develop three algorithms, based on a shelling method, which give recommendations for optimal sphere-packings. We interpret these packings as treatment plans, and we examine the corresponding radiation dosages for various qualities.

We analyze the effectiveness of our algorithms in recommending optimal dosage plans. Several problems with the algorithms are addressed. Finally, we conclude that all of our algorithms have a common difficulty covering very large tumors, and that while one of our algorithms is effective as a means of packing the volume with spheres, it does not translate into an efficient treatment plan.

Introduction

The gamma knife is a highly effective means of destroying tumor tissue. A collection of 201 beams, which send ionizing radiation produced by cobalt-60 sources, converge and deliver to a specific region a powerful dose of radiation without harming the surrounding tissue.

It is necessary to determine where the beams should converge, so the patient's brain is scanned with an MRI or CT imaging device to produce a three-dimensional image of the tumor. An optimal treatment plan is determined by analyzing this image and deriving a collection of points inside the tumor. Doses concentrated at those points are administered by the gamma knife. Selecting an optimum treatment plan can be lengthy and difficult.

We seek to automate the process of selecting an optimal treatment. We describe an algorithm to take a three-dimensional image and determine an

The UMAP Journal 24 (3) (2003) 365–378. ©Copyright 2003 by COMAP, Inc. All rights reserved. Permission to make digital or hard copies of part or all of this work for personal or classroom use is granted without fee provided that copies are not made or distributed for profit or commercial advantage and that copies bear this notice. Abstracting with credit is permitted, but copyrights for components of this work owned by others than COMAP must be honored. To copy otherwise, to republish, to post on servers, or to redistribute to lists requires prior permission from COMAP.

optimal choice for the position and size of spheres that cover the tumor as much as possible while the same time minimizing the number of spheres utilized.

The basic ingredients of our solution include:

- three tumor growth models representing three different degrees of nonuniformity;
- three sphere-packing algorithms, each representing a different spin on the concept of “shelling”; and
- testing of the algorithms against three different tumor sizes.

Exploring the Layout of the Problem

Collimators

A collimator helmet is used to direct the radiation toward a specific point in the patient’s head. Cobalt-60 as a radiation source emits photons in an isotropic fashion; so, by introducing a long cylinder between the source and the target, the beams are constrained to a certain angular distribution. Over the short distance from the end of the cylinder to the target location, the radiation is confined approximately to a cylinder or column. This collimation of the radiation allows specific targeting and reduced exposure.

The collimator helmet is essentially a spherical array of cylinders, each of which directs radiation through a common point. This configuration allows 201 low-intensity beams to enter the brain and intersect in one well defined location. Since the beams are positioned around the skull evenly and are relatively weak, no normal tissue receives a high dose. However, where the beams intersect in the tumor, a huge dose is delivered (**Figure 1**). Because the collimator has only four different settings, we are physically restricted to four different dose sizes.

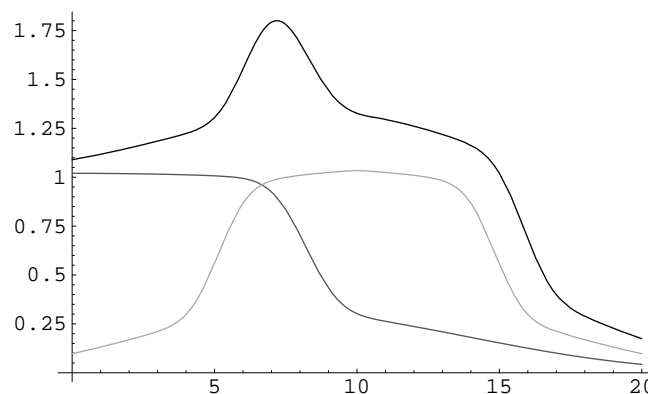


Figure 1. Radiation profile where spheres meet. The bottom two curves represent radiation profiles for individual shots (radii of 7 and 4 centered at 0 and 11) and the bold line represents the total radiation dose received.

Radiation Distribution

Because the cobalt-60 sources are evenly spaced, their intersection can be represented by a spherically symmetric radiation profile. This profile can be approximated well by error functions [Ferris and Shepard 2000]. Thus, we define the radial distribution of dose intensity to be

$$f_{\rho}(d) = \sum_{i=1}^2 \lambda_i \left[1 - \operatorname{erf} \left(\frac{d - r_i}{\sigma_i} \right) \right], \quad (1)$$

where λ_i , σ_i , and r_i all depend on ρ , the radius of the sphere, and d is the distance from the center of the sphere. By fitting the values of λ , σ , and r to experimental data, an accurate model for radiation intensity is generated. Ferris and Shepard [2000] give fitted values for radii of various sizes.

It is impractical to design an algorithm to optimize the placement of such intersections (called *shots*) over multiple treatments. Thus, a placement method must be developed that is both accurate and quick. By approximating the shots from collimator helmets as spheres, a much more approachable problem may be formulated: How can we pack the tumor with as many spheres as possible? By using spheres of the same radius as the beams, we agree very well with the drop-off point of the radiation distribution defined above. Thus, by packing the tumor, we can optimize the placement and number of shots.

Isosurfaces and Isodose

The constructs that define habitability within our brain space are the isodose surfaces, or *isosurfaces*. These surfaces are the level sets of the scalar field that makes up the radiation distribution in the brain space. Every point on one side of the surface has a higher dosage than any point on the other. In an ideal case, the edge of the tumor would be the isodose surface, with every point inside the tumor receiving 100% of the prescribed radiation and every point not in the tumor receiving none. However, this is infeasible, so some compromise must be reached. By comparing the regions within isosurfaces to the tumor, it is easy to see how much tumor has been cleared away, how much tumor is left, and how much brain has been sacrificed.

Digital Images of Tumors

Typically, an MRI delivers an image of the brain case, with a resolution of approximately 1 mm^3 . Since the brain is about 100 mm on a side, the tumor image sits inside a $100 \times 100 \times 100$ voxel space, where each voxel represents 1 mm^3 . We assume that the shape given by the imaging software is an accurate and conservative approximation of the tumor, so that if we subject voxels denoted as tumorous to doses of radiation do not damage normal brain tissue.

Problem Restatement

Given these considerations, we may restate the problem before us as follows. Given a digital image of tumor tissue, produce a list of at most 15 spheres (centers and radii) such that:

- The spheres are entirely contained within the tumor tissue.
- Each radius is either 2, 4, 7, or 9 mm.
- The spheres are disjoint (or nearly so, to avoid overdosing).
- The total volume of the spheres is as close to that of the tumor as possible.

Tumor Generation Model

We could not find images of actual tumors, so we generated our own. We created an algorithm to simulate tumor growth in time steps. This algorithm uses a cellular automaton to model cellular division [Kansal 2000]. Ideally, the lattice would have a structure similar to a biological fabric, but we take instead a simple three-dimensional grid, for several reasons:

- It is computationally convenient—not only is simulation elementary, but the output resembles a digital image without further processing.
- We are interested in studying the final shape of tumors, not their growth. Our algorithm is sufficient to produce volumes representative of tumor shapes.

Each node of the lattice represents an idealized mathematical cell. We begin by placing a single cell in the center of the space, allowing the cells to “divide” (generate a new cell) at each time step until the tumor reaches the desired size. Whether or not a cell divides depends on several factors, which vary among the three different generation methods discussed below.

In all cases, we smooth out unrealistic or undetectable holes in the tumor after it has grown to the desired size. It is theoretically possible for a tumor to reconnect with itself in a toroidal shape, but this does not happen in practice.

The Uniform Pressure Tumor

This simulation supposes that the tumor is growing in a uniformly pressurized environment. At each time step, the probability for a given cell to divide is proportional to $(1 - r/R)$, where r is the distance from the cell to the origin and R is a bound on the radius of the tumor. Since we are interested only in the final tumor shape and not its development, the constant of proportionality is essentially irrelevant. The resulting tumor shape is generally a ragged sphere.

The Varied Pressure Tumor

Suspecting that the preceding model may be too symmetric, we created a second algorithm that varies the pressure against the tumor, corresponding to the effect that the surrounding area of the brain would have on the growth of a tumor. To do this, we specify certain random points x_i as pressure points and curb tumor growth near these points. The probability for a given cell x to divide is now proportional to the product $(1 - r/R) \prod |x - x_i|/M$, where M is the maximum width of the tumor space and r and R are as before.

Tumors generated with this model are slightly more elongated and pointed than before. Some curve into a lima-bean shape around the pressure points.

The Running Amok Tumor

Newman and Lazareff [2002] postulate that once a tumor begins to jut in one direction, cells in the outcropping are more likely to receive nutrients from the surrounding brain tissue and hence are more likely to grow, whereas the less extended regions of the tumor are less likely to grow. The tumor is more likely to grow in a direction in which it has grown before; the result is a tumor that is spiny in appearance. Thus, in this third model, we remove the outside pressures and specify that more recently generated cells be more likely to divide than older ones. The resulting shape is a bulky tumor with tendrils showing recent and active growth.

Packing Spheres into Volumes

The sphere-packing problem is ages old and yet unsolved; the very problem that we are faced is NP-complete [Wang 1999].

When faced with packing rounds into a barrel, the military has been rumored to pack them as tightly as possible and then drive the barrel in a large truck over a bumpy road; doing so clears up enough space for another handful of rounds. We implement an algorithmic approximation to this idea.

The General Approach

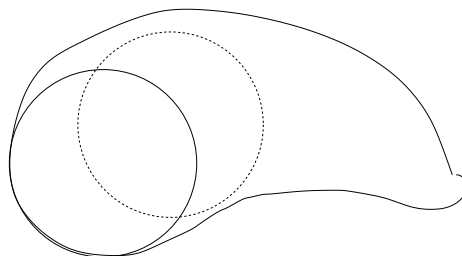
Our plan is based on two fundamental principles:

Fit the largest spheres first. That is, we pack large spheres into the volume before considering smaller ones. The reason for this is the steep fall-off of coverage as shot radius decreases (**Table 1**). It takes twice as many 7-mm spheres to do the job of a 9-mm sphere, consuming more diametric space in the tumor and complicating the dosage plan. Since one of our stated goals is to minimize the number of doses, the principle of utilizing larger spheres first is clearly a good one.

Table 2.

Shot radius vs. coverage.

Radius (mm)	9	7	4	2
Coverage (mm ³)	3000	1300	250	12

**Figure 2.** The sphere on the left is a better choice than the one on the right.

Spheres should hug the tumor edge. It is very likely for there to be a many-way tie for where to place the largest sphere that fits inside a given volume. But not all choices are equal—a centrally placed sphere may preclude fitting other large spheres into the volume (**Figure 2**). For example, it would be unwise to place a 9-mm shot at the center of a spherical tumor that is 16 mm in radius, as this would not allow us to place any 7-mm spheres into the tumor.

Depth-Search Algorithm

Because the tumor data is in the form of a digital image, we pack spheres into the image directly. That is, we select spherical subsets of voxels from the given tumor and consider the optimal placing of spheres (centered at voxels inside the tumor) that do not intersect one other or the edge of the tumor.)

The algorithm acts by a *shelling method* [Wagner et al. 2000], which we describe in detail. The first step is to identify the boundary of the tumor, marking the voxels on a bounding surface with value of 0. We then assign every tumorous voxel a positive value, denoting its distance from the boundary nodes, via **Algorithm 1**.

The sphere that we place inside the tumor should be as large as possible but also as close to the boundary as possible. We therefore take for the center of this sphere a point at depth r from the boundary, where r is the greatest of 2, 4, 7, and 9 available. This way, when we shell a sphere at depth r , the shelled area is along the edge of the tumor as much as possible.

In any case, our algorithm must choose the center x of the sphere from the set E_r . How this is done varies among the three algorithms.

Having chosen our candidate shell center x , we remove from the tumor the sphere centered at the center of this voxel of radius r . This translates to removing all voxels in the tumor whose coordinates are within r of the center

Algorithm 1 The depth evaluation algorithm

```

 $X$  is the set of tumorous voxels
 $E_0$  is the set of boundary voxels
 $d := 0$ 
while  $X \neq \emptyset$  do
  for  $x \in X$  do
    if  $x$  neighbors a point of  $E_d$  then
      move  $x$  from  $X$  to  $E_{d+1}$ 
    end if
  end for
  increment  $d$ 
end while

```

of the sphere.

We iteratively apply this shelling method to the volume of tumor that remains. The algorithm terminates after it has shelled 15 times, since that is the maximum number of shots allowed. However, we keep track at each stage of what percentage of the tumor has been eliminated so that fewer shots may be recommended if they are deemed sufficient.

A Hasty Algorithm

This is the simplest algorithm. Each time we must choose a center for our shell of radius r , we simply grab one at random. In some sense, this algorithm acts as a control for the next two.

A Careful Algorithm

This next algorithm improves upon the previous one in an obvious way. At each stage, we select a candidate center x from the set E_r —one that will be most beneficial toward placing the remaining spheres. Since the placement of the largest spheres has the greatest effect on the percentage of the volume, we determine which choice of center results in the largest depth by applying the shelling process to what remains of the tumor after the sphere centered at that point has been removed. We want the remaining region to have as high a depth as possible, to make it more likely that we can fit large spheres in the surrounding area.

While it would be preferable to compare all possible choices, to do so is in most cases too computationally intensive. We therefore select a number of our centers in E_r (in this case, 5), compute in each case the depth of the volume of the tumor minus the sphere centered at that point, and from these 5 pick the one whose remaining tumor has voxels with the highest depth.

A Wiggling Algorithm

Prototyping these two algorithms revealed that our Depth-Search algorithm does not always choose sphere centers as close to the tumor boundary as possible.

We developed the Wiggling algorithm as a partial solution to this problem. It rests on the theory that the depth algorithm may still work to find spheres that hug the boundary closely.

The Wiggling algorithm chooses a voxel x from E_r at random and places inside the tumor a sphere of radius r centered at the voxel. It then transports the sphere, one unit at a time, starting off in a random direction and continuing until the sphere meets the boundary as closely as possible. That is, the algorithm simply transports the sphere until it discovers that the next step would land it outside the tumor. By no accident, this method very much resembles that truck on a bumpy road.

Unfortunately, the methods of this algorithm cannot be combined efficiently with the previous Careful algorithm; any care exerted would simply be undone by wiggling.

Output

One cannot distinguish from the three-dimensional images the differences among our three algorithms. **Figure 3** shows a cut-away plot of tumor wall, together with 15 spheres selected by the Careful algorithm.

Analyzing Sphere-Placement Plans

Computing Dose Distributions

After completing calculations using discrete spheres and voxel models of tumors, we calculate the actual dose distribution from the proposed treatment plan. Using the centers of the spheres and the radially symmetric radiation functions presented earlier, we construct a scalar field in brain space defined by the formula

$$D(x, y, z) = \sum_{i=1}^n f_{r_i}(\sqrt{(x - x_i)^2 + (y - y_i)^2 + (z - z_i)^2}),$$

where f is the function given in (1) on p. 361 and (x_i, y_i, z_i) is the center of the i th sphere with radius r_i .

For all (x, y, z) in a voxel, we use the center of the voxel. Thus, all the points in the voxel get the value of D at the center, and the values of D are thereby discretized. Of course, it would be more accurate to integrate over the entire cube and use the computed value as the representative number for

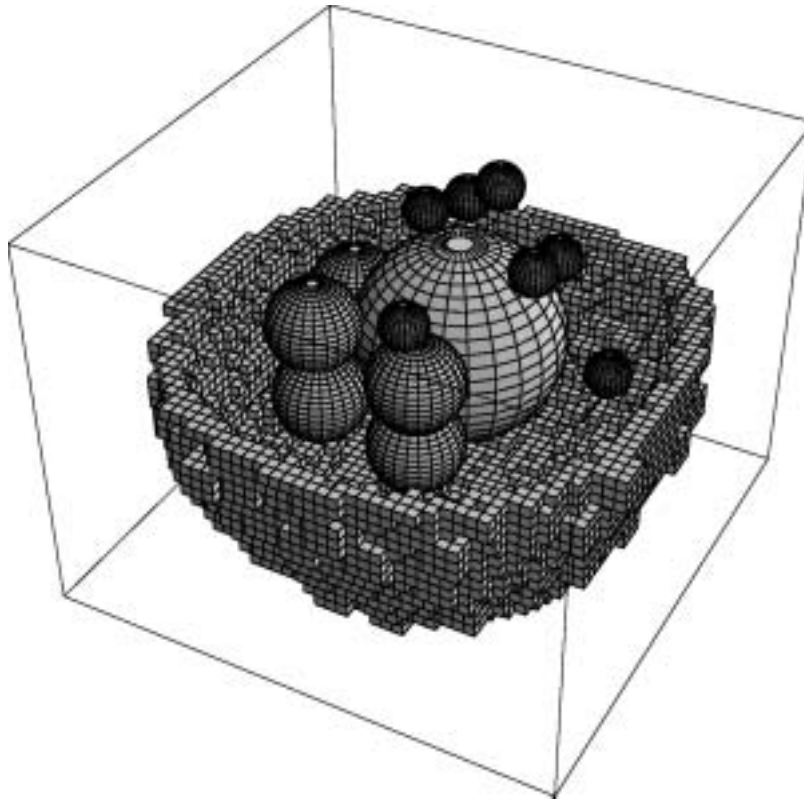


Figure 3. Spheres packed in a tumor by the Careful algorithm.

the voxel, but this is too computationally intensive and the accuracy gained on test cases was minimal. Using this scalar field, we can calculate isosurfaces of any value and the volume of the region contained in this isosurface. By taking various different isosurfaces, the efficiency of the spherical covering plan can be calculated. The amount of damage to the surrounding tissue is also available.

Determining the Number of Shots

Each step in our algorithm is executed in the same way whether or not there will be a subsequent shot. Hence, computing every shot and then using some set of parameters to determine the value of each successive shot enables us to compute the ideal number of shots for each tumor. Since this method is not incredibly time consuming (10–15 min for a large tumor). It is certainly feasible to run this process in the hospital and deliver a dose profile to a patient in moments.

Visualizing Dose Distribution

To facilitate visualization of dose distribution, we construct a program to slice the field of dose distribution and superimpose an image of the tumor

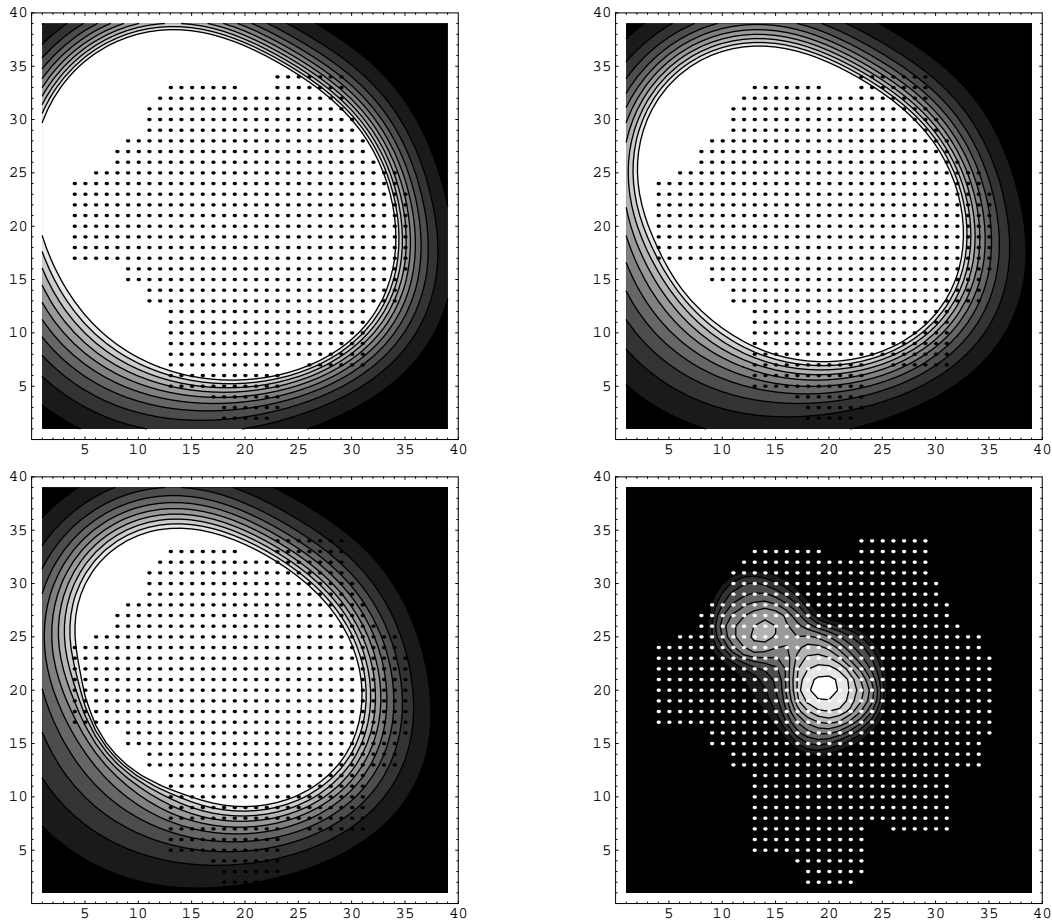


Figure 4. A single cross-sectional slice of a tumor (represented by dots). Top-left: 30% cut-off. Top-right: 50% cut-off. Bottom-left: 80% cut-off. Bottom-right: Shows only hot spots.

on it (**Figure 4**). Multiple slices make it possible to see a three-dimensional isosurface profile of the tumor. The white areas in the images of **Figure 4**, from top-left clockwise, are the regions of the tumor that receive a radiation dosage above 30, 50, 80%, and the region of potential overdosing, i.e., a region with an intensity higher than 2.5 times that of a single shot, referred to as a *hotspot*.

Applying the Algorithm

We are allowed a maximum of 15 spheres. In all of our simulations, it was possible to place 15 spheres inside the tumors, since they were of relatively high volume compared to a sphere, especially to a sphere of radius 2 mm.

From each of our three tumor-growth models, we produced 30 tumor images, 10 each of sizes $10,000 \text{ mm}^3$, $20,000 \text{ mm}^3$, and $36,000 \text{ mm}^3$. We then tested each of the three algorithms against all 90 tumors.

We performed two operations:

- We used the spherical dose pattern to create a scalar field of radiation expo-

sure values throughout the $100 \times 100 \times 100$ brain space. We then used this field to calculate the exposures of every cell within the modeled brain and tumor and to decide which cells survived the treatment. Using a 30% contour as our cutoff for death and survival, and further calculating the percentage exposures to other isodose cutoff values, we obtained exposure percentages for various tumor shapes and sphere-placement algorithms (**Table 2**).

Table 2. Percentage of tumor receiving 30/40/50% of shot intensity.
Best results for a tumor shape and size are shown in bold.

Shape	Size (mm ³)		
	10,000	20,000	36,000
a. Hasty algorithm.			
Uniform	96/86/71	96/86/68	96/86/68
Varied	95/82/70	96/89/70	76/69/54
Amok	94/87/70	91/82/63	78/66/49
b. Careful algorithm.			
Uniform	96/85/69	98/91/70	99/92/73
Varied	99/96/84	92/82/69	92/86/72
Amok	94/85/64	88/79/62	79/66/50
c. Wiggling algorithm.			
Uniform	99/95/82	91/83/69	88/81/67
Varied	99/96/84	92/82/69	92/86/72
Amok	91/85/72	79/71/56	76/65/51

- We took the spherical profiles generated by the placement algorithms and estimated the radiation exposure values to all of the brain space for each generation of spherical dose pattern created by the algorithm. When the total dosage of the tumor reached a specified value, in this case 30%, the spherical dose profile of that generation was recorded. Thus, the total number of shots delivered to the patient is minimized while maintaining effective coverage of the tumor. Reducing this data gives **Table 3**. A dash means that the algorithm could not fill 90% of the volume with 15 spheres.

Evaluation of Methods and Conclusions

Difficulties Reaching 90% Coverage

Even for simple volumes, it can be impossible to cover 90% of a tumor with shots. To see this, consider a sphere of 10 mm radius. We may shell this with a

Table 3. Approximate number of shots needed to kill 90% of the tumor.
Best results for a shape and size of tumor are shown in bold.

Shape	Volume (mm ³)		
	10,000	20,000	36,000
a. Hasty algorithm.			
Uniform	8	15	7
Varied	15	10	9
Amok	10	–	–
b. Careful algorithm.			
Uniform	7	12	7
Varied	–	12	9
Amok	10	–	–
c. Wiggling algorithm.			
Uniform	10	10	15
Varied	9	11	15
Amok	15	–	–

9-mm sphere, which would leave no room even for a 2-mm sphere and would still cover less than 3/4 of the volume.

Simply put, the only way our algorithms can destroy 90% of the tumors is by allowing hotspots in the tumor.

Square Lattices vs. Euclidean Distance

Even worse, no instance of our algorithm can see that it is possible to put a 9-mm shot in the 10-mm sphere. This is because the depth evaluation algorithm assigns depths to the tumorous voxels that do not entirely correspond to the physical distance between the voxels and the tumor edge. In **Figure 5** (at left), when voxels happen to differ via the coordinate axes, then the depth differential coincides with the distance between the voxels. However, in every other case the depth does not quite accurately measure distance. For example, two voxels that are diagonally adjacent differ in depth by 1, whereas the Euclidean distance between the centers of the two voxels is $\sqrt{3}$.

In many situations, the shelling method gives centers a depth that is not an accurate representation of their position inside the tumor. For example, in **Figure 5** (at right), the highlighted voxel has depth 3; so if we choose that voxel as the center of our circle, then we would place a circle of radius 3 at that point to cover the tumor. But it is clearly possible to squeeze a circle of radius 4 into the tumor. The problem is exaggerated further in three dimensions.

Our Wiggling algorithm was developed as an attempt to find a partial so-

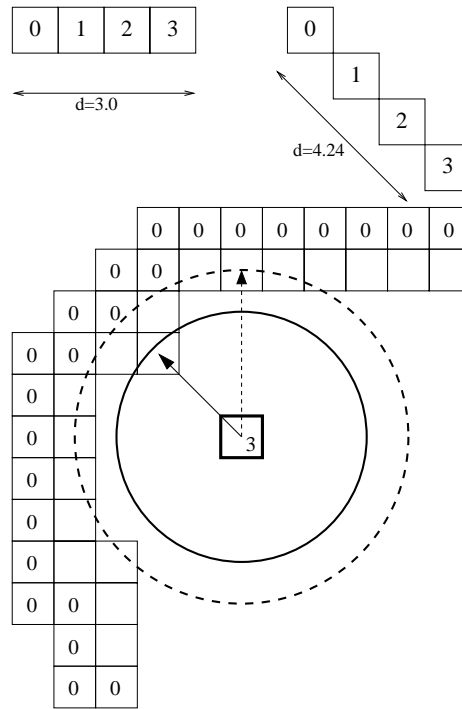


Figure 6. Left: Metric inconsistencies. Right: A schematic highlighting a weakness of our depth model.

lution to this problem. By allowing the spheres to move toward the edge of the tumor, we hoped to pack the spheres as tightly as possible.

Conclusion/Recommendation

For small or medium-sized tumors, the Careful algorithm is comparable to the Hasty Algorithm; the Hasty algorithm is preferable on time considerations.

All of the algorithms, but especially the Wiggling algorithm, have difficulty handling very large tumors, ones so large compared to the sphere sizes that it is unlikely that any combination of spheres could fill the volume of the tumor to the degree required by the problem statement.

However, for reasonably-sized tumors, the Wiggling algorithm is quite effective and works especially well toward filling in the varied-pressure tumors. This is because they bulge around the pressure points, forming pockets that are ideal for nesting spheres. When the spheres wiggle, they are more likely to settle into these regions and thus pack tightly. Furthermore, the Wiggling method runs much faster, especially compared to the Careful algorithm.

In fact, the Wiggling algorithm does such a good job of packing spheres that if we do not constrain the total number of spheres used, it tends to pack a very many, resulting in a large dosage. Furthermore, since the spheres are packed to the edge, the radiation spills out of the tumor into the surrounding normal tissue. So, while the Wiggling algorithm is a very good method of sphere-packing, it is not good for treatment planning.

To summarize:

- None of these algorithms should be used for very large tumors, which should be treated in multiple sessions.
- For moderate-sized tumors, the Hasty algorithm should be used in preference to the Careful algorithm.
- The Wiggling method is speedy and effective but does not translate well into an effective and safe treatment plan. However, we recommend it for tumors similar in shape to varied-pressure tumors, because it produces optimal plans for those.

References

- Ferris, Michael C., and David M. Shepard. 2000. Optimization of gamma knife radiosurgery. In *Discrete Mathematical Problems with Medical Applications*, vol. 55 of DIMACS Series in Discrete Mathematics and Theoretical Computer Science, edited by D.-Z. Du, P. Pardolas, and J. Wang, 27–44. Providence, RI: American Mathematical Society. <ftp://ftp.cs.wisc.edu/pub/dmi/tech-reports/00-01.pdf>.
- Kansal A.R., S. Torquato, G.R. Harsh, E.A. Chiocca, and T.S. Deisboeck. 2000. Simulated brain tumor growth dynamics using a three-dimensional cellular automaton. *Journal of Theoretical Biology* 203 (4): 367–382.
- McKernan, R.O., and G.D. Wilde. 1980. Mathematical models of glioma growth. In *Brain Tumors*, edited by D.G.T. Thomas and D.I. Graham. London, UK: Butterworth & Co.
- Newman, William I., and Jorge A. Lazareff. 2002. A mathematical model for self-limiting brain tumors. <http://www2.ess.ucla.edu/~newman/LGA.pdf>.
- Wagner, Thomas H., et al. 2000. A geometrically based method for automated radiosurgery planning. *International Journal of Radiation, Oncology, Biology, Physics* 48 (5): 1599–1611.
- Wang, Jie. 1999. Packing of unequal spheres and automated radiosurgical treatment planning. *Journal of Combinatorial Optimization* 3: 453–463.
- Wu, Q. Jackie. 2000. Sphere packing using morphological analysis. In *Discrete Mathematical Problems with Medical Applications*, vol. 55 of DIMACS Series in Discrete Mathematics and Theoretical Computer Science, edited by D.-Z. Du, P. Pardolas, and J. Wang, 27–45. Providence, RI: American Mathematical Society.